European Radiology (2019) 29:1144–1152
https://doi.org/10.1007/s00330-018-5686-6

UROGENITAL

Accessory cavitated uterine mass: MRI features and surgical correlations of a rare but under-recognised entity

N. Peyron[1] · E. Jacquemier[1] · M. Charlot[1] · M. Devouassoux[2,3] · D. Raudrant[3,4] · F. Golfier[3,4] · P. Rousset[1,3]

Received: 26 April 2018 / Revised: 9 July 2018 / Accepted: 27 July 2018 / Published online: 29 August 2018

Abstract

Objectives To describe MRI features of accessory cavitated uterine mass (ACUM) with surgical correlations.

Methods Eleven young women with an ACUM at pathology underwent preoperative pelvic MRI. Two experienced radiologists retrospectively analysed MR images in consensus to determine the lesion location within the uterus, its size, morphology (shape and boundaries), and structure reporting the signal and enhancement of its different parts compared to myometrium. The presence of an associated urogenital malformation or other gynaecological anomaly was reported. MRI features were correlated with surgical findings.

Results All 11 lesions were well correlated with surgical findings, lateralised (seven were left-sided), and located under the horn and the round ligament insertion. Nine were located within the external myometrium, bulging into the broad ligament. Two were extrauterine, entirely located within the broad ligament. On MRI, the mean size was 28 mm (range 17–60 mm). Nine lesions were round-shaped, two were oval; all had regular boundaries. At surgery, the ACUM were not encapsulated but were possible to enucleate. On MRI, all lesions were well defined and showed a central haemorrhagic cavity surrounded by a regular ring (mean thickness, 5 mm) which had the same signal compared to the junctional zone. ACUM was isolated in all women, without urogenital malformation, adenomyosis or deep endometriosis.

Conclusions On MRI, ACUM was an isolated round accessory cavitated functional non-communicating horn-like aspect in an otherwise normal uterus. MRI may facilitate timely diagnosis and appropriate curative fertility-sparing laparoscopic resection.

Key Points

- *ACUM is rare, with delayed diagnosis in young women with severe dysmenorrhoea. Pelvic MRI facilitates timely diagnosis and appropriate curative fertility-sparing laparoscopic resection.*
- *Quasi-systematically located under the uterine round ligament insertion, ACUM may be intramyometrial and/or in the broad ligament.*
- *On MRI ACUM resemble a non-communicating functional accessory horn within a normal uterus; the mass, most often round-shaped, had a central haemorrhagic cavity surrounded by a regular ring which had the same low signal compared to the uterine junctional zone.*

Keywords Uterine anomalies · Magnetic resonance imaging · Dysmenorrhoea · Pelvic pain · Adenomyosis

Electronic supplementary material The online version of this article (https://doi.org/10.1007/s00330-018-5686-6) contains supplementary material, which is available to authorized users.

✉ P. Rousset
roussetpascal@gmail.com

[1] Radiology Department, Lyon Sud University Hospital, Hospices Civils de Lyon, 165 Chemin du Grand Revoyet, 69495 Pierre Bénite, France

[2] Pathology Department, Lyon Sud University Hospital, Hospices Civils de Lyon, Lyon, France

[3] Lyon 1 Claude Bernard University, Lyon, France

[4] Gynaecology and Obstetrics Department, Lyon Sud University Hospital, Hospices Civils de Lyon, Lyon, France

Abbreviations

ACUM	Accessory cavitated uterine mass
ESHRE	European Society of Human Reproduction and Embryology
ESGE	European Society for Gynaecological Endoscopy
FOV	Field of view
MR	Magnetic resonance
MRI	Magnetic resonance imaging
OR	Oestrogen receptor
PR	Progesterone receptor
ST	Section thickness
TE	Echo time
TR	Repetition time

Introduction

Since the first description by Oliver in 1912 [1], the literature converges to a new type of Müllerian abnormality probably related to dysfunction of the female gubernaculum, previously called juvenile or isolated cystic adenomyoma [2–6], uterus-like mass [7] or accessory uterine cavity [8], and recently regrouped under the term accessory cavitated uterine mass (ACUM) by Acién et al [9–16]. This rare entity is defined by the presence of a non-communicating accessory uterine mass found in the uterus or within the broad ligament, close to the round ligament insertion, with an otherwise normal genital tract [3, 5, 9, 10]. At pathology, it is characterised by a central cavity lined by functional endometrium, often filled with chocolate-coloured blood, and surrounded by a ring of smooth muscle [1, 9, 10, 17]. Although rare, it may also be underdiagnosed as clinical diagnosis is non-specific and misleading, with a delayed final diagnosis [9, 10, 14, 15]. Patients are mostly teenagers or young nulliparous women (< 30 years) and present clinical manifestations such as severe dysmenorrhoea, recurrent pelvic pain and abdominal cramps, which are rapidly progressive after menarche and become resistant to analgesic drugs [10]. Pain is often on the ipsilateral side of the mass and persists or even increases after menstruation. Positive diagnosis is problematic because of the broad differential diagnosis that includes all causes of dysmenorrhoea, particularly pelvic endometriosis, but also uterine mass or malformation when a mass is palpated at physical examination.

In this context, imaging work-up is pivotal for early correct diagnosis of ACUM, and to provide preoperative mapping to guide conservative management. However, most knowledge of imaging features is derived from three radiological case reports [2, 4, 14] or succinct imaging descriptions in clinical series [5, 6, 9, 10]. Thanks to its high reliability and accuracy, magnetic resonance imaging (MRI) is currently the imaging modality of choice to achieve complete exploration of female genital anomalies [18, 19].

The purpose of this retrospective study, conducted in a referral centre for gynaecological diseases, was to describe MRI findings and surgical correlations in women with pathologically proven ACUM.

Materials and methods

The study protocol received institutional review board approval, which waived requirement for informed consent, and was in accordance with the 1964 Helsinki declaration and later amendments.

Patients

Between October 2011 and October 2017, the retrospective search of our institutional electronic database yielded 11 women who underwent surgery, had pelvic MRI within 6 months before surgery (meeting standards agreed to by the investigators) and had pathologically proven ACUM.

Clinical history was collected, including age, gravity and parity, preoperative clinical symptoms, such as dysmenorrhoea and pelvic pain, and effectiveness of medical treatments, as were post-operative symptoms over at least 6 months.

MRI protocol

MRI data were obtained at our institution (6/11) or elsewhere (5/11) and digitised into our image archiving and communication system (Centricity PACS; GE Medical Systems).

At our institution, MRI were acquired on a 1.5-Tesla MRI unit (Achieva until 2013 and Ingenia thereafter; Philips Medical Systems) using pelvic phased-array coils for signal reception, after intravenous administration of 1 mg glucagon (1 mg/mL, GlucaGen; Novo Nordisk). Each examination on MRI unit (n = 5) included at least axial, coronal and sagittal T2-weighted turbo spin-echo images (repetition time (TR) 1080–3550 ms/echo time (TE) 105 ms; section thickness (ST), 4 mm; field of view (FOV), 20–23 cm), axial T1-weighted spin-echo images (TR 560 ms/TE 10 ms; ST, 3 mm; FOV, 22 cm), axial fat-suppressed T1-weighted images (TR 655 ms/TE 15 ms; ST, 3 mm; FOV, 20.5 cm). With the exception of two MR examinations, axial and sagittal fat-suppressed T1-weighted images (TR 505–710 ms/TE 7.5–14 ms; ST, 4 mm; FOV, 230–250 mm) were acquired after intravenous administration of gadoterate meglumine (0.2 mL/kg body weight, Multihance; Bracco).

All five external MR examinations, performed at four different imaging centres, using at least 1.5-Tesla MRI units, phased-array surface coils and acquisition of T2-weighted images in two planes, axial T1-weighted spin-echo images and/or axial fat-suppressed T1-weighted images. Among these five women, three also had intravenous administration of contrast agent sequences.

All women had a kidney exploration using US or during pelvic MRI.

MRI image analysis

Two readers (P.R. and M.C., with 10 and 8 years' experience in gynaecological imaging, respectively) reviewed in consensus all MR examinations on viewing workstations (View forum, Philips Medical Systems), blinded to clinical information except that the women had surgery for an ACUM.

A standardised data collection form was used to report ACUM MRI findings based on adapted pathological and surgical descriptions [9, 10, 17] as summarised in Table 1 and as follows: ACUM location within the uterus including uterine site, uterine level (fundus was defined as the uterine part located above the line passing between the two horns), and myometrial location (ACUM located within the myometrium were reported using the FIGO leiomyoma subclassification system [20], and the thickness of normal myometrium between the uterine cavity and the ACUM was also collected); ACUM morphology; ACUM structure, including the presence or absence of a central cavity and peripheral ring (T1-weighted and T2-weighted signal, and enhancement if available, were compared to outer myometrium [21]).

The presence of a normal uterus (normal endometrial lumen, two normal horns) or associated Müllerian malformation was also collected, as was the presence or absence of myometrial (adenomyosis, myoma), adnexal abnormalities, pelvic endometriosis or associated kidney malformation.

Surgery

Two surgeons experienced in uterine malformation management (D.R. and F.G.) performed surgical procedures. All non-virgin women underwent hysteroscopy first and then laparoscopy under general anaesthesia. Hysteroscopy was performed to rule out Müllerian duct anomaly and identify a potential submucous component of the lesion. The peritoneal cavity was explored to confirm the localisation of the mass, check the normal appearance of adnexa and exclude differential diagnosis. The ACUM was then removed; the uterine serosa and broad ligament were incised anteriorly, then passing around the mass to make a conservative progressive focal excision of the myometrium when needed, without opening the uterine cavity. Intrauterine methylene blue injection in non-virgin women demonstrated no communication between the uterine cavity and surgical site. From surgical reports, the level and laterality, the uterine site, the myometrial location and the size of the ACUM were retrospectively collected.

Pathological examination

Macroscopic analysis of the excised surgical specimen demonstrated a round or oval cavitated mass with a central cavity filled with a haemorrhagic chocolate-brown-coloured liquid when not opened by surgeons. Histological sections were stained with haematoxylin–eosin–saffron, and immunohistochemical stainings were performed for markers of normal endometrial stroma such as CD10, oestrogen receptor (OR) and progesterone receptor (PR). Microscopic examination of the cavity lining found normal-appearing and well-organised endometrial-like tissue (with CD10, OR and PR positivity of the endometrium-like stroma), surrounded by a layer of myometrium-like smooth muscle with a concentric organisation around the cavity [10, 17].

Results

Patients

Mean age at diagnosis was 21 years (range 14–28 years), all women were nulligravida and had history of severe dysmenorrhoea, or severe pelvic pain following menstruation and/or chronic pelvic pain. Pain was lateralised in 7/11 women, always the side of the ACUM. Before surgery, 8/11 women received medication for this pain (3/11 NSAID, 4/11 oral contraceptive with oestroprogestogen or progestogen only, and 1/8 GnRH agonist). None had complete resolution of pain, but the woman who received a GnRH agonist reported partial resolution.

Mean follow-up was 23 months (range 6–72 months) and all women remained pain-free, without significant dysmenorrhoea and had normal cycles. No pregnancy after surgery was reported during the study period.

Table 1 Summary of the data collection form used to report ACUM MRI findings

Location within the uterus			Morphology	Structure	
Site	Level	Myometrial location		Central cavity	Peripheral ring
Midline	Fundus	Within the myometrium	Size in millimetres	Diameter in millimetres	Thickness in millimetres
Paramedian	Body	Within the broad ligament	Shape—round or oval	T1W and T2W SI	T1W and T2W SI, and enhancement, if available
Lateral	Cervix	–	Boundaries—regular or irregular	Presence of inner lining	–

T2W SI T2-weighted signal intensity, *T1W SI* T1-weighted signal intensity

MRI findings with surgical correlations

ACUM location within the uterus

On MRI, all 11 ACUM were single and lateralised (seven were left-sided); they were located under the horn and the round ligament insertion (Table 2). Nine were located in the uterus body within the external myometrium (outside the junctional zone) and partly bulging into the broad ligament. Among the latter, six were less than 50% intramural (FIGO type 6) (Figs. 1 and 2 and Electronic Supplementary Material (ESM) Fig. 1); three were at least 50% intramural (FIGO type 5) (ESM Fig. 2). These nine partly intramyometrial ACUM were distant from the uterine cavity; the mean myometrial interface thickness was 6 mm (range 2–10 mm), consistent with the absence of uterine cavity opening during ACUM removal. Two of the 11 ACUM were extrauterine under the horn, entirely located within the broad ligament (Fig. 3). Laparoscopy confirmed MRI features. In 9/11 women, the surgeon found a lateralised intramyometrial mass (4/9 right, 5/9 left), bulging into the broad ligament. In two women, the surgeon found a mass that had developed within the left broad ligament.

ACUM morphology

On MRI, the mean diameter of the ACUM was 28 mm (range 17–60 mm), and when measured at surgery or pathology (n = 9/11) this was 28 mm (range 20–60 mm). Nine lesions were round, two were oval; all had regular boundaries. At surgery, the ACUM were not encapsulated but were clearly delineated from the surrounding myometrium or broad ligament and possible to enucleate. The nine lesions with intramyometrial component required myometrial dissection to be removed (Fig. 1). The two located in the broad ligament were directly removed with a smooth surface at macroscopic examination (Fig. 3).

ACUM structure

On MRI, all ACUM were found to have a central cavity, the mean diameter of which was 24.5 mm (range 9–52 mm). All cavities showed high T1 signal intensity that was persistent after fat saturation, and in 10 a T2 shading effect. The latter corresponded to intermediate signal intensity in eight ACUM (a fluid-fluid level in four of these) (Figs. 1 and 2, ESM Figs. 1 and 2), and a low signal intensity T2 in two ACUM (Fig. 3). At surgical or pathological macroscopic examinations, all ACUM had a central cavity filled with a haemorrhagic chocolate-brown-coloured liquid (Fig. 3). In 6/11 ACUM, the cavity was lined by a thin inner lining that moderately enhanced after gadolinium administration and had an aspect similar to endometrium; in 4/6 of these there was a slight hypersignal on T2-weighted images (Fig. 2, ESM Fig. 1). Each central cavity was surrounded by a well-defined ring

Table 2 ACUM MRI characteristics of the 11-case series

Case	Age (years)	Size (mm)	Location			Morphology		Central cavity			Inner lining			Peripheral ring			
			Side	Level	Relative to myometrium	Shape	Boundaries	Diameter (mm)	T2W SI	T1W SI	Present	T2W SI	Enhancement	Thickness (mm)	T2W SI	T1W SI	Enhancement
1	23	31	L	Body	BL	Round	Regular	15	Low	High	Y	UD	Mild	8	Low	Low	Low
2	22	60	R	Body	FIGO 6*	Oval	Regular	52	Inter	High	Y	High	Mild	4	Low	Low	Low
3	14	19	R	Body	FIGO 5*	Round	Regular	13	Inter	High	N	NA	NA	3	Low	Low	NA
4	22	26	R	Body	FIGO 6*	Round	Regular	16	Inter	High	Y	UD	Mild	5	Low	Low	Low
5	21	27	L	Body	FIGO 6*	Round	Regular	19	Inter	High	Y	High	Mild	4	Low	Low	Low
6	22	25	R	Body	FIGO 6*	Round	Regular	13	High	High	N	NA	NA	6	Low	Low	NA
7	22	17	L	Body	FIGO 5*	Round	Regular	9	Inter	High	Y	High	Mild	4	Low	Low	Low
8	15	18	L	Body	BL	Round	Regular	12	Low	High	N	NA	NA	3	Low	Low	NA
9	26	44	L	Body	FIGO 6*	Oval	Regular	36	Inter	High	Y	High	Mild	5	Low	Low	Low
10	17	21	L	Body	FIGO 6*	Round	Regular	12	Inter	High	N	NA	NA	6	Low	Low	NA
11	28	28	L	Body	FIGO 5*	Round	Regular	13	Inter	High	N	NA	NA	7	Low	Low	NA

T2 and T1 signals are given compared to the outer myometrium

T2W SI T2-weighted signal intensity, *T1W SI* T1-weighted signal intensity, *R* right, *L* left, *BL* broad ligament, *NA* not applicable, *Y* yes, *N* no, *Inter* intermediate, *UD* undetectable, *NA* non applicable

*Intramyometrial location using classification derived from the FIGO leiomyoma subclassification system

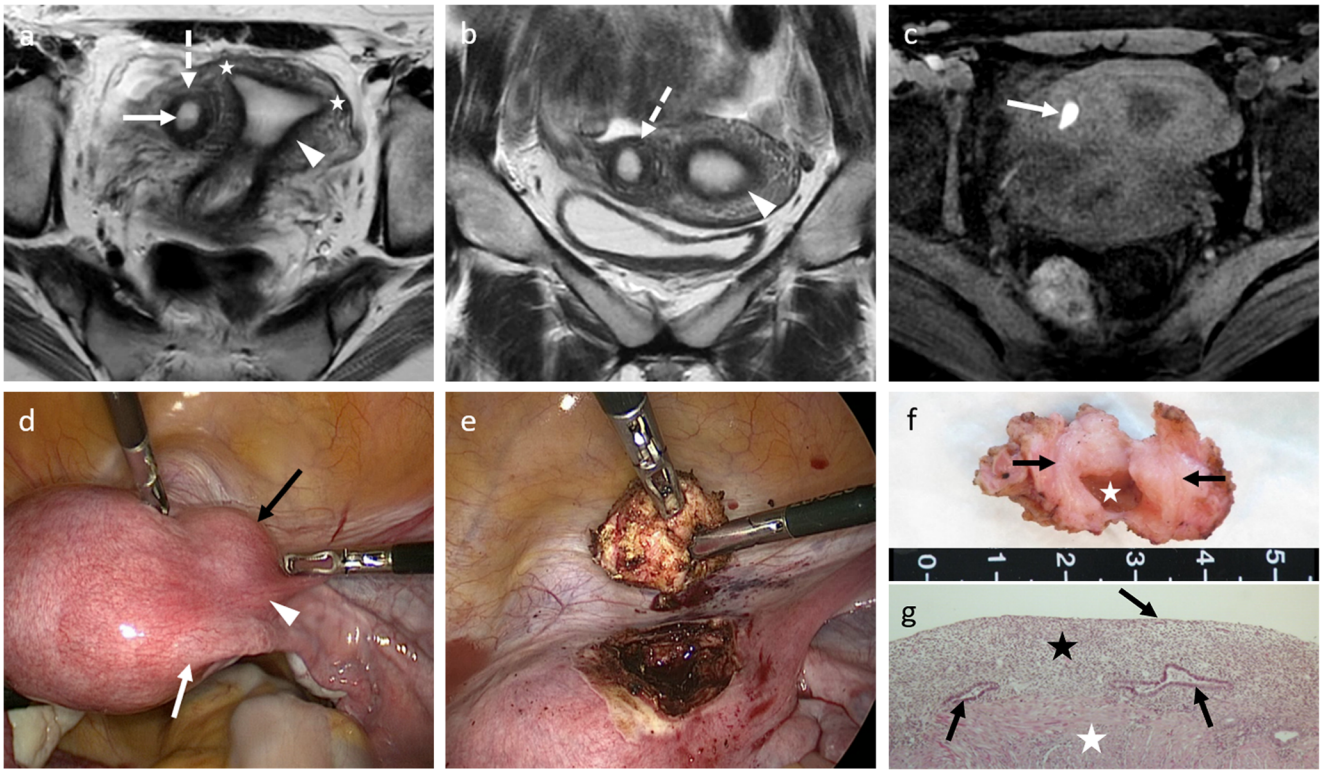

Fig. 1 Case 4, a 22-year-old woman with catamenial gradually worsening right-sided pelvic pain. Axial (**a**) and coronal (**b**) T2-weighted MRI images show the presence of a focal round cavitated mass of 26-mm width, right-sided in the outer myometrium of the uterus, in subserosal position bulging into the broad ligament (FIGO type 6), with a central fluid level (arrow) and surrounded by a low T2 signal ring (dashed arrows), identical to the junctional zone (arrowheads). Note the normal uterine cavity, with two horns (stars), distinct from the cavitated mass. **c** Axial T1-weighted MRI image with fat saturation shows a high T1 signal in the central cavity suggesting haemorrhagic content (arrow). **d** Laparoscopic view shows a uterine right-sided mass bulging into the anterior part of the broad ligament (FIGO type 6) (black arrow) located under the horn and tubal insertion (white arrow), just under the insertion of the round ligament (arrowhead). **e** Laparoscopic view shows the mass after excision from the myometrium. **f** Macroscopic examination of the open mass shows a cavitated mass (star) surrounded by a thick concentric wall (arrows). **g** Histological photography of the mass (haematoxylin and eosin stain, original magnification ×5) shows an endometrium at the cavity side, composed of a columnar epithelium at its surface or delimiting glands (arrows) and stroma (black star), lining a thick peripheral layer of concentric smooth muscle of myometrium type (white star)

(mean thickness 5 mm, range 3–8 mm) with low T1 and T2 signal (Figs. 1, 2, and 3, and ESM Figs. 1 and 2) and low enhancement (n = 7/11) compared to the outer myometrium (Fig. 2 and ESM Fig. 1). This MRI pattern was similar to that of the junctional zone (also known as the inner myometrium).

In all women the uterine cavity had a normal shape on MRI, which was consistent with that seen with hysteroscopy. No woman had an associated congenital uterine or kidney anomaly. No associated adenomyosis, myoma or deep endometriosis was reported. Two women had paraoophoritic cysts and one had a contralateral small hydrosalpinx, secondarily confirmed at surgery. For two women a few small superficial endometriotic pelvic implants were found at surgery.

Discussion

The present study reports that MRI findings of ACUM correlated with surgical findings and its pathological definition [1, 9, 10, 17], appearing as a round cavitated mass filled with haematometra with an inner lining and surrounded by a regular ring similar to the junctional zone. On the basis of these findings, and previous MRI descriptions of uterine horn in Müllerian abnormality [18, 22], an ACUM could be defined on MRI as a functioning and non-communicating accessory horn, present within the external myometrium and/or in broad ligament in an otherwise normal uterus. These findings were consistent and reproducible in all women of the study and seem to correlate with the few imaging case reports and MRI images available in clinical series of ACUM [2, 4, 9, 10, 14]. The MRI description of ACUM herein could thus complete the definition that was initially based on clinical, surgical and pathological findings, and thus adds to the growing body of data arguing for a separate new type of Müllerian abnormality, as proposed by Acién et al [11, 12]. This may also lead one to better individualise this entity within the U6 class of the European Society of Human Reproduction and Embryology (ESHRE)/European Society for Gynaecological

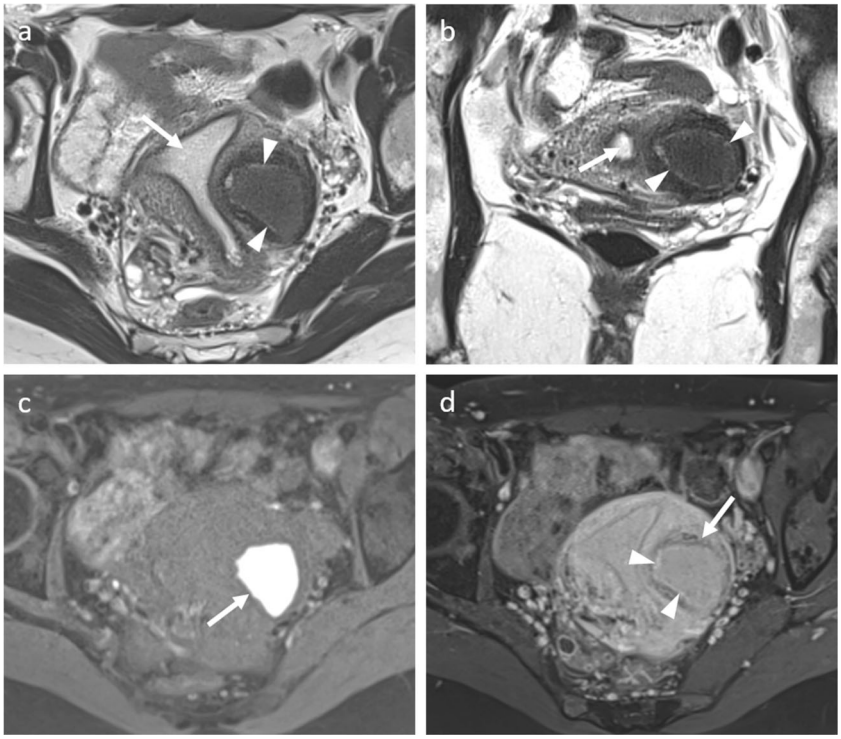

Fig. 2 Case 9, a 26-year-old woman with severe dysmenorrhoea. Axial (**a**) and coronal (**b**) T2-weighted MRI images show the presence of a large oval left-sided mass in the outer myometrium of the uterus, mostly bulging into the broad ligament (FIGO type 6), with an intermediate signal central cavity surrounded by a low T2 signal ring. The cavity is delineated by a slightly hyperintense thin inner lining (arrowheads), similar to endometrium (arrows). **c** Axial T1-weighted MRI image shows high T1 signal in the central cavity (arrow). **d** Axial contrast-enhanced fat-saturated T1-weighted MRI image shows mild enhancement of the inner lining (arrowheads) and low enhancement of peripheral ring (arrow) compared to the surrounding outer myometrium and identical to the junctional zone

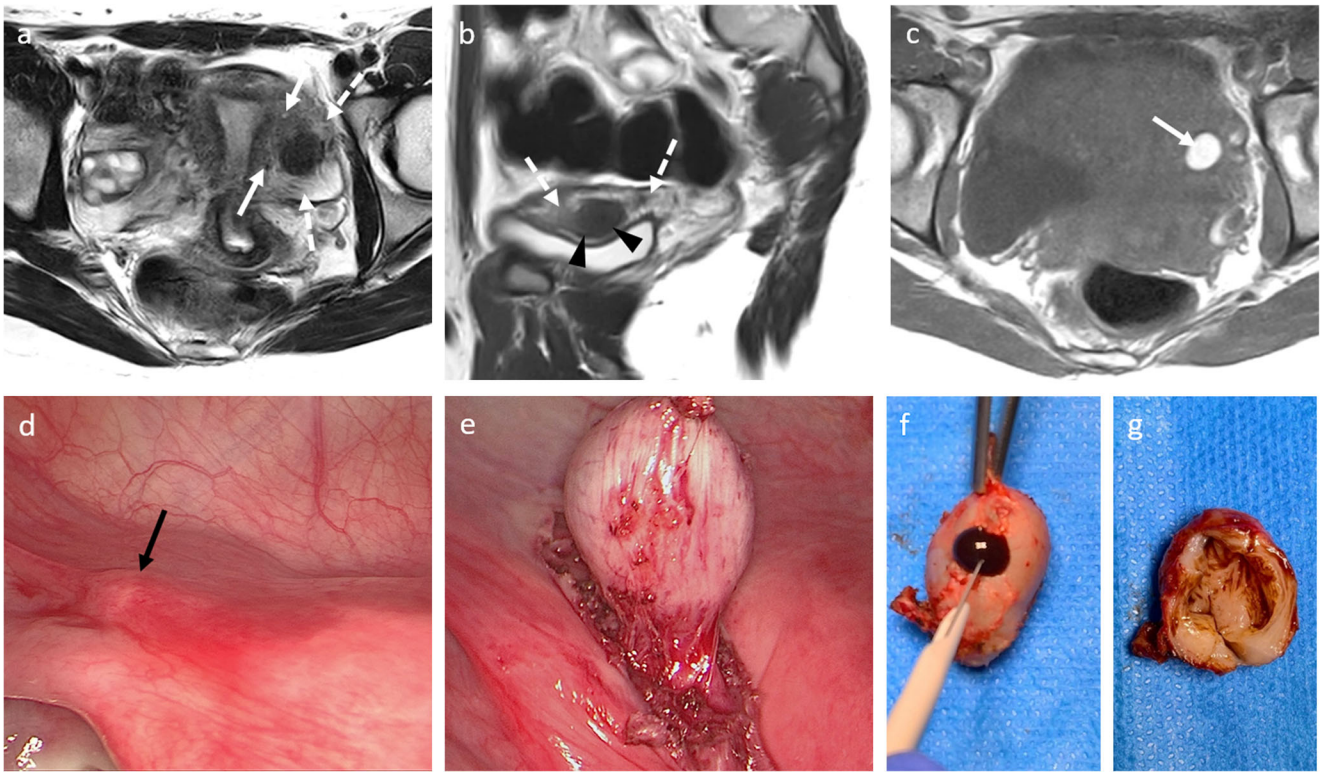

Fig. 3 Case 8, a 15-year-old woman with severe dysmenorrhoea and left-sided chronic pelvic pain, resistant to NSAID. Axial (**a**) and sagittal (**b**) T2-weighted MRI images show a well-circumscribed low signal mass located within the left broad ligament (dashed arrows), bulging on is anterior face (arrowheads) and demarked from the outer myometrium (arrows). **c** Axial T1-weighted MRI image shows high T1 signal in the central cavity suggesting haemorrhagic content (arrow). **d** Laparoscopic view of the mass bulging on the surface of the anterior part of the left broad ligament (arrow). **e** Laparoscopic view shows the mass easily enucleated from the broad ligament. Note the smooth borders of the lesion. **f** The macroscopic view of the extracted mass shows a flow of chocolate-coloured fluid from the cavity at the point of incision, consistent with blood. **g** The macroscopic view of the opening mass shows a cavitated mass with a muscular wall

Endoscopy (ESGE) classification that includes unclassified cases, and which is designed to include cases resulting from formation, fusion or absorption defects of normal embryological developments as well as ectopic Müllerian tissue anomalies [23].

ACUM is less rare than previously believed, making the consideration of an ACUM diagnosis essential in clinically suspicious cases. However, diagnosis of ACUM is challenging because of the lack of specificity of its clinical picture, making imaging work-up pivotal to assess the positive diagnosis and rule out others [6, 10]. Transvaginal ultrasonography is an accessible first-line imaging examination but needs an experienced radiologist. Moreover, women with an ACUM are often very young and sometimes virgin at the time of diagnosis. Pelvic MRI, considered as the reference technique for pelvic examination, also seems suitable to better explore ACUM thanks to its contrast resolution that may best depict the layered ACUM components [18, 19]. On the basis of the results presented herein, the pelvic MRI protocol classically recommended in uterine malformation (at least two orthogonal T2-weighted sequences and an axial fat-suppressed T1-weighted sequence) can be used and should be sufficient to make positive diagnoses [18]. Gadolinium may be helpful to depict the endometrium underlying the ACUM cavity but was not essential to make the diagnosis in our experience. While kidney exploration is recommended in cases of Müllerian duct malformation, no kidney abnormalities have been described to be associated with ACUM [11, 12].

The present report may be helpful to better identify ACUM; yet in the context of pelvic pain with a uterine mass on imaging, some differential diagnoses have to be ruled out. First of all, previously termed juvenile or isolated cystic adenomyoma in young women should be regrouped with ACUM to avoid nosological framework overlap, as proposed by Acién et al [9–16]. Moreover, adenomyosis in its organised and cystic form, called cystic adenomyoma, may have some significant differences to ACUM in terms of clinical, surgical pathological findings as well as imaging findings reported herein [24–26]. Adenomyosis mostly affects older, multiparous women [24–26]. Adenoyoma is commonly found in association with other adenomyotic lesions in the uterus and has no systematic or preferential topography, although it is mostly reported within or contiguous to the junctional zone. Its margins are irregular and undefined [25, 26]. Cystic components are frequent, usually found as multiple and small (< 5 mm) areas spread in the adenomyotic lesions, and very rarely as a unique central cavity as systematically found herein [25, 26]. At pathological examination, a cystic adenomyoma is composed of endometrial glands surrounded by endometrial-type stroma and smooth muscle, but lacks the uterus-like organisation that is found in ACUM [17]. In ACUM there is a concentric organisation of smooth muscle around ectopic endometrium, which was also depicted on MRI in some cases herein [17]. Another differential diagnosis could be the non-communicating rudimentary horn of a unilaterally formed uterus, with haematometra (class U4a of the ESHRE/ESGE classification) [23]. The key finding is the oblong uterine cavity with abnormal unique horn, whereas ACUM is found within an otherwise normally shaped uterus with two horns [18, 27]. As has been the case in Müllerian abnormalities [18, 22], the results presented herein suggest that MRI may avoid hysterosalpingography that is recommended by some authors for the diagnosis of ACUM to rule out the possibility of a communicated cavitated rudimentary uterine horn [11, 12]. Ovarian endometrioma found close to the broad ligament could also mimic ACUM as a result of the haemorrhagic content in the context of lateralised cyclic pelvic pain [27]. However, endometrioma is located in the ovary, is easily found by following the ovarian vessels or with the adjacent presence of follicles, and certainly does not have any thick peripheral ring of muscular tissue. In some cases, a leiomyoma with a large central cystic degeneration may be radiologically confused with ACUM, but these affect older women and the clinical context is different as myomas are not particularly responsible for cyclic menstrual pain. Multiple leiomyomas are commonly found, only 2% are solitary and have no preferential topography [28]. A cystic degeneration occurs in only 4% of leiomyomas [29]. Such cystic leiomyomas are well defined, with a residual peripheral ring of smooth muscle, but their content is rarely haemorrhagic [30].

MRI could allow timely positive diagnosis in women experiencing pain and prompt treatment to relieve symptoms. Hormone therapy using GnRH agonists or oral contraceptives can be proposed, but symptoms may not be completely relieved and usually rapidly recur at the end of therapy [5]. The most effective therapeutic approach to prevent the typical relentless suffering of these young women is considered to be tumourectomy, which should preferentially be performed laparoscopically [3, 5, 6]. ACUM occurs in young women, for whom fertility preservation is a priority. A precise preoperative MRI mapping of the ACUM may be useful to guide the surgeon to select the most appropriate site for the uterine incision, favouring a laparoscopic approach to perform conservative surgery; this increases safety, allows fertility-sparing excision and lowers the risk of rupture related to uterus scarring in future pregnancies. Moreover, using the FIGO subclassification for leiomyoma to describe the location of the ACUM within the myometrium as proposed herein, the surgeon may better anticipate the depth of the penetration in the myometrium to remove the ACUM. This is less complicated than for adenomyoma for which there is no surgical removing plane, as ACUM borders are delineated from normal myometrium allowing enucleation without extensive myometrial damage [5, 6].

The present study does have some limitations. Namely, the sample size is small, which is related in part to the inclusion of

women with preoperative MRI and surgically resected ACUM secondarily confirmed by pathological examination. However, this does ensure accurate image–pathology correlation, and the study population is at least comparable to that of reference gynaecological studies [5, 9, 10]. In addition, MRI images were acquired on different 1.5-Tesla MRI units and with variable MRI protocols, but standard sequences for pelvic analysis were performed in all women, and did not alter the accurate MRI image analysis.

In conclusion, this study reports that MRI findings of ACUM seem well correlated with surgical and pathological features, depicting an isolated round accessory functional non-communicating horn-like aspect in an otherwise normal uterus. The MRI diagnosis of ACUM may facilitate timely diagnosis and provide a useful precise mapping of the ACUM for appropriate, curative, safe and fertility-sparing laparoscopic resection.

Acknowledgements The authors would like to thank Philip Robinson (DRCI, Hospices Civils de Lyon) for help in manuscript preparation.

Funding: The authors state that this work has not received any funding.

Compliance with ethical standards

Guarantor The scientific guarantor of this publication is Professor Pascal Rousset, Lyon, France.

Conflict of interest The authors of this manuscript declare no relationships with any companies whose products or services may be related to the subject matter of the article.

Statistics and biometry No complex statistical methods were necessary for this paper.

Informed consent Written informed consent was waived by the institutional review board.

Ethical approval Institutional review board approval was obtained.

Methodology
- retrospective
- observational
- performed at one institution

References

1. Oliver J (1912) An accessory uterus distended with menstrual fluid enucleated from the substance of the right broad ligament. Lancet 179:1609
2. Kataoka ML, Togashi K, Konishi I et al (1998) MRI of adenomyotic cyst of the uterus. J Comput Assist Tomogr 22:555–559
3. Takeda A, Sakai K, Mitsui T, Nakamura H (2007) Laparoscopic management of juvenile cystic adenomyoma of the uterus: report of two cases and review of the literature. J Minim Invasive Gynecol 14:370–374
4. Ho ML, Raptis C, Hulett R, McAlister WH, Moran K, Bhalla S (2008) Adenomyotic cyst of the uterus in an adolescent. Pediatr Radiol 38:1239–1242
5. Takeuchi H, Kitade M, Kikuchi I, Kumakiri J, Kuroda K, Jinushi M (2010) Diagnosis, laparoscopic management, and histopathologic findings of juvenile cystic adenomyoma: a review of nine cases. Fertil Steril 94:862–868
6. Kriplani A, Mahey R, Agarwal N, Bhatla N, Yadav R, Singh MK (2011) Laparoscopic management of juvenile cystic adenomyoma: four cases. J Minim Invasive Gynecol 18:343–348
7. Liang YJ, Hao Q, Wu YZ, Wu B (2010) Uterus-like mass in the left broad ligament misdiagnosed as a malformation of the uterus: a case report of a rare condition and review of the literature. Fertil Steril 93:1347.e13–1347.e16
8. Potter DA, Schenken RS (1998) Non communicating accessory uterine cavity. Fertil Steril 70:1165–1166
9. Acién P, Acién M, Fernández F, José Mayol M, Aranda I (2010) The cavitated accessory uterine mass: a Müllerian anomaly in women with an otherwise normal uterus. Obstet Gynecol 116:1101–1109
10. Acién P, Bataller A, Fernández F, Acién MI, Rodríguez JM, Mayol MJ (2012) New cases of accessory and cavitated uterine masses (ACUM): a significant cause of severe dysmenorrhea and recurrent pelvic pain in young women. Hum Reprod 27:683–694
11. Acién P, Sánchez del Campo F, Mayol MJ, Acién M (2011) The female gubernaculum: role in the embryology and development of the genital tract and in the possible genesis of malformations. Eur J Obstet Gynecol Reprod Biol 159:426–432
12. Acién P, Acién MI (2011) The history of female genital tract malformation classifications and proposal of an updated system. Hum Reprod Update 17:693–705
13. Bedaiwy MA, Henry DN, Elguero S, Pickett S, Greenfield M (2013) Accessory and cavitated uterine mass with functional endometrium in an adolescent: diagnosis and laparoscopic excision technique. J Pediatr Adolesc Gynecol 26:e89–e91
14. Jain N, Verma R (2014) Imaging diagnosis of accessory and cavitated uterine mass, a rare mullerian anomaly. Indian J Radiol Imaging 24:178–181
15. Paul PG, Chopade G, Das T, Dhivya N, Patil S, Thomas M (2015) Accessory cavitated uterine mass: a rare cause of severe dysmenorrhea in young women. J Minim Invasive Gynecol 22:1300–1303
16. Peters A, Rindos NB, Guido RS, Donnellan NM (2018) Uterine-sparing laparoscopic resection of accessory cavitated uterine masses. J Minim Invasive Gynecol 25:24–25
17. World Health Organization (2003) World Health Organization classification of tumours: pathology and genetics of tumours of the breast and female genital organs. World Health Organization, Geneva http://www.iarc.fr/en/publications/pdfs-online/pat-gen/bb4/. Accessed 10 Jul 2018
18. Behr SC, Courtier JL, Qayyum A (2012) Imaging of mullerian duct anomalies. Radiographics 32:E233–E250
19. Grimbizis GF, Di Spiezio Sardo A, Saravelos SH et al (2016) The Thessaloniki ESHRE/ESGE consensus on diagnosis of female genital anomalies. Hum Reprod 31:2–7
20. Munro MG, Critchley HO, Broder MS, Fraser IS, FIGO Working Group on Menstrual Disorders (2011) FIGO classification system (PALM-COEIN) for causes of abnormal uterine bleeding in nongravid women of reproductive age. Int J Gynaecol Obstet 113:3–13
21. Lakhman Y, Veeraraghavan H, Chaim J et al (2017) Differentiation of uterine leiomyosarcoma from atypical leiomyoma: diagnostic accuracy of qualitative MR imaging features and feasibility of texture analysis. Eur Radiol 27:2903–29152
22. Hall-Craggs MA, Williams CE, Pattison SH, Kirkham AP, Creighton SM (2013) Mayer-Rokitansky-Kuster-Hauser syndrome: diagnosis with MR imaging. Radiology 269:787–792

23. Grimbizis GF, Gordts S, Di Spiezio Sardo A et al (2013) The ESHRE/ESGE consensus on the classification of female genital tract congenital anomalies. Hum Reprod 28:2032–2044
24. Parazzini F, Vercellini P, Panazza S, Chatenoud L, Oldani S, Crosignani PG (1997) Risk factors for adenomyosis. Hum Reprod 12:1275–1279
25. Tamai K, Togashi K, Ito T, Morisawa N, Fujiwara T, Koyama T (2005) MR imaging findings of adenomyosis: correlation with histopathologic features and diagnostic pitfalls. Radiographics 25:21–40
26. Bazot M, Daraï E (2018) Role of transvaginal sonography and magnetic resonance imaging in the diagnosis of uterine adenomyosis. Fertil Steril 109:389–397
27. Chamié LP, Blasbalg R, Pereira RM, Warmbrand G, Serafini PC (2011) Findings of pelvic endometriosis at transvaginal US, MR imaging, and laparoscopy. Radiographics 31:E77–E100
28. Bazot M, Deux JF, Dahbi N, Chopier J (2001) Myometrium diseases. J Radiol 82:1819–1840
29. Moyle PL, Kataoka MY, Nakai A, Takahata A, Reinhold C, Sala E (2010) Nonovarian cystic lesions of the pelvis. Radiographics 30: 921–938
30. Protopapas A, Milingos S, Markaki S et al (2008) Cystic uterine tumors. Gynecol Obstet Invest 65:275–280